

Arrestin 1 and Cone Arrestin 4 Have Unique Roles in Visual Function in an All-Cone Mouse Retina

Janise D. Deming,¹ Joseph S. Pak,¹ Jung-a Shin,^{1,2} Bruce M. Brown,¹ Moon K. Kim,³ Moe H. Aung,⁴ Eun-Jin Lee,^{1,5} Mabelle T. Pardue,^{3,4} and Cheryl Mae Craft^{1,6}

¹Mary D. Allen Laboratory for Vision Research, Department of Ophthalmology, Keck School of Medicine of the University of Southern California, USC Eye Institute, Los Angeles, California, United States

²Department of Anatomy, School of Medicine, Ewha Womans University, Seoul, Korea

³Rehabilitation Research & Development Center of Excellence, Atlanta VA Medical Center, Decatur, Georgia, United States

⁴Neuroscience/Ophthalmology, Emory University, Atlanta, Georgia, United States

⁵Department of Biomedical Engineering, University of Southern California Viterbi School of Engineering, Los Angeles, California, United States

⁶Department of Cell & Neurobiology, Keck School of Medicine of the University of Southern California, Los Angeles, California, United States

Correspondence: Cheryl Mae Craft, USC Eye Institute, Department of Ophthalmology, Keck School of Medicine of the University of Southern California, IGM, 2250 Alcazar Street, Mail Code: 9075, Clinical Sciences Center 135H, Los Angeles, CA 90033, USA; CherylMae.Craft@med.usc.edu, eyesightresearch@hotmail.com.

JDD and JSP contributed equally to the work presented here and should therefore be regarded as equivalent authors.

Submitted: July 30, 2015

Accepted: October 13, 2015

Citation: Deming JD, Pak JS, Shin J, et al. Arrestin 1 and cone arrestin 4 have unique roles in visual function in an all-cone mouse retina. *Invest Ophthalmol Vis Sci.* 2015;56:7618-7628. DOI:10.1167/iovs.15-17832

PURPOSE. Previous studies discovered cone phototransduction shutoff occurs normally for *Arr1*^{-/-} and *Arr4*^{-/-}; however, it is defective when both visual arrestins are simultaneously not expressed (*Arr1*^{-/-}*Arr4*^{-/-}). We investigated the roles of visual arrestins in an all-cone retina (*Nrl*^{-/-}) since each arrestin has differential effects on visual function, including ARR1 for normal light adaptation, and ARR4 for normal contrast sensitivity and visual acuity.

METHODS. We examined *Nrl*^{-/-}, *Nrl*^{-/-}*Arr1*^{-/-}, *Nrl*^{-/-}*Arr4*^{-/-}, and *Nrl*^{-/-}*Arr1*^{-/-}*Arr4*^{-/-} mice with photopic electroretinography (ERG) to assess light adaptation and retinal responses, immunoblot and immunohistochemical localization analysis to measure retinal expression levels of M- and S-opsin, and optokinetic tracking (OKT) to measure the visual acuity and contrast sensitivity.

RESULTS. Study results indicated that *Nrl*^{-/-} and *Nrl*^{-/-}*Arr4*^{-/-} mice light adapted normally, while *Nrl*^{-/-}*Arr1*^{-/-} and *Nrl*^{-/-}*Arr1*^{-/-}*Arr4*^{-/-} mice did not. Photopic ERG a-wave, b-wave, and flicker amplitudes followed a general pattern in which *Nrl*^{-/-}*Arr4*^{-/-} amplitudes were higher than the amplitudes of *Nrl*^{-/-}, while the amplitudes of *Nrl*^{-/-}*Arr1*^{-/-} and *Nrl*^{-/-}*Arr1*^{-/-}*Arr4*^{-/-} were lower. All three visual arrestin knockouts had faster implicit times than *Nrl*^{-/-} mice. M-opsin expression is lower when ARR1 is not expressed, while S-opsin expression is lower when ARR4 is not expressed. Although M-opsin expression is mislocalized throughout the photoreceptor cells, S-opsin is confined to the outer segments in all genotypes. Contrast sensitivity is decreased when ARR4 is not expressed, while visual acuity was normal except in *Nrl*^{-/-}*Arr1*^{-/-}*Arr4*^{-/-}.

CONCLUSIONS. Based on the opposite visual phenotypes in an all-cone retina in the *Nrl*^{-/-}*Arr1*^{-/-} and *Nrl*^{-/-}*Arr4*^{-/-} mice, we conclude that ARR1 and ARR4 perform unique modulatory roles in cone photoreceptors.

Keywords: visual arrestins, NRL knockout, cone opsins, cone function

Visual arrestins are responsible for shutting off the G-protein coupled receptor (GPCR)-light-activated cascades of phototransduction in rods and cones. Arrestin 1 (ARR1, S-antigen, or 48 kD protein)¹⁻³ is highly expressed in rods,⁴⁻⁶ pinealocytes,⁶ and mouse cones.⁷ Arrestin 4 (ARR4, cone arrestin [CAR]) is highly expressed in mammalian cones and pinealocytes.⁸

The primary mechanism of action of ARR1 in rods has been the subject of intense study. After light activation, rhodopsin is phosphorylated multiple times by G-protein coupled receptor kinase 1 (GRK1)^{9,10} and subsequently bound by ARR1.^{2,11-13} Binding of ARR1 to the GPCR effectively shuts off further rhodopsin signaling by inhibiting further interaction with the α subunit of its cognate G-protein, transducin.

The phenotype of *Arr1*^{-/-} mice has demonstrated clearly the necessity of this protein for rod phototransduction shutoff^{12,14} and light adaptation,¹⁵ though single-cell cone photoreceptor electrophysiological shutoff is normal in these mice.⁷ Furthermore, ARR1 is highly expressed in mouse cones and it can substitute for ARR4 in the cone phototransduction shutoff pathway,⁷ although transgenic mice with ARR4 expressed in rods lacking ARR1 display deficits in the known functions of ARR1,¹⁶ including phototransduction shutoff,¹² light adaptation,¹⁵ and synaptic function.¹⁷

The concentration of ARR4 in mouse cones is approximately 2% of the total arrestin concentration while the other 98% is arrestin 1, yet at the single-cell level, cone shutoff

kinetics are approximately the same in *Arr1*^{-/-} and *Arr4*^{-/-}.⁷ This indicates that ARR4 has a much higher affinity for cone opsins than ARR1, and has an important role in the termination of the light-activated signal that originates with the cone opsins. Mice lacking both ARR1 and ARR4 display a lack of rod and cone phototransduction shutoff and are unable to light-adapt normally.^{7,15}

The evolutionary conservation of ARR4^{7,18,19} suggests that it has an important role in maintenance of cone structure and function that is not redundant with that of ARR1, and recent evidence clearly supports this idea.²⁰ The zebrafish ortholog of ARR4 in red/green cones was shown to be essential for normal contrast sensitivity in zebrafish larvae.²¹ In addition, visual defects in *Arr4*^{-/-} mice compared to WT, including decreases in contrast sensitivity, visual acuity, and a slow age-related cone dystrophy, have been reported.²⁰ These phenotypes are distinct from those observed in *Arr1*^{-/-} mice,^{7,12,14,15} indicating that ARR4 performs a unique role in cones, the mechanisms of which have yet to be discovered. Based on these results, we hypothesized that ARR1 and ARR4 perform differing roles aside from phototransduction shutoff in mouse cones.

Because of the rod-dominance of mouse retinas with greater than 97% rods, it is difficult to assess the role of ARR1 in cones with commonly used strains of mice. In these mice, nearly all of the ARR1 is located in rods, and removing ARR1, as in the *Arr1*^{-/-} mouse, primarily affects the rod-driven phenotypes of the mice. In addition, *Arr1*^{-/-} mice must be dark-reared to prevent light-dependent degeneration of the rods and, eventually, cones.¹⁴ The dark-rearing of these mice may have a deleterious effect on their retinal and visual development and light-driven modulation of their circadian rhythms, impacting the observed visual phenotypes.

To avoid these issues and to achieve a greater focus on cone-specific function, we used an established mouse model that lacks rods and has an “all-cone” retina, the neural retina leucine zipper knockout (*Nrl*^{-/-}). The *Nrl* gene encodes a transcription factor that is essential for rod development.²²⁻²⁴ When normal mice are genetically engineered and the *Nrl* gene is knocked out, rod progenitor cells differentiate into short-wavelength sensitive cones (S-cones).²⁵ In humans, genetic mutations in the *NRL* gene can result in autosomal dominant retinitis pigmentosa (adRP).^{26,27} The *Nrl*^{-/-} mouse model²⁵ has been an invaluable tool for investigating cone function in mice,²⁸⁻³¹ isolating cone-specific proteins,³² or both.³³⁻³⁸ Taking advantage of the all-cone phenotype, investigators have created other genetically engineered mice strains by backcrossing mice with *Nrl*^{-/-} to investigate the role of other specific cone expressed genes in cone function.^{29,33,36-38}

To compare and contrast the roles of the two visual arrestins, ARR1 and ARR4, in an all-cone mouse retina, we compared the following four genotypes of mice: *Nrl*^{-/-}, *Nrl*^{-/-}*Arr1*^{-/-}, *Nrl*^{-/-}*Arr4*^{-/-}, and *Nrl*^{-/-}*Arr1*^{-/-}*Arr4*^{-/-}. Based on previous work, we hypothesized that *Nrl*^{-/-}*Arr1*^{-/-} and *Nrl*^{-/-}*Arr4*^{-/-} would display normal cone phototransduction shutoff but have unique visual phenotypes because ARR1 and ARR4 perform different roles in the cone photoreceptors. In addition, we hypothesized that the triple-knockout mice, *Nrl*^{-/-}*Arr1*^{-/-}*Arr4*^{-/-}, would have a third, more severe phenotype than either of the double-knockout mice because, lacking visual arrestins, its cone phototransduction shutoff is defective.

To test our hypotheses, we used the methods of electroretinography (ERG) to reveal the electrophysiological signaling properties of the all-cone mouse retinas without ARR1, ARR4, or either expressed; we measured expression levels and examined immunohistochemical localization of M- and S-opsin

in each genotype, and we used optokinetic tracking (OKT) to determine whether any defects observed result in behavioral or functional consequences for vision in mice.

METHODS

Mice

We originally produced *Arr4*^{-/-} mice in our laboratory on a mixed C57Bl/6J-129SVJ strain (WT) background (details in supplement⁷); *Arr1*^{-/-} mice¹² were generously provided by Jeannie Chen (University of Southern California [USC]); *Arr1*^{-/-}*Arr4*^{-/-} mice⁷ were produced by backcrossing the two strains together; *Nrl*^{-/-} mice²⁵ were generously provided by Anand Swaroop (National Eye Institute [NEI], Bethesda, MD, USA) and bred with each visual arrestin knockout strain to produce *Nrl*^{-/-}*Arr4*^{-/-}, *Nrl*^{-/-}*Arr1*^{-/-}, and *Nrl*^{-/-}*Arr1*^{-/-}*Arr4*^{-/-}. The genotypes of all breeding pairs and their offspring were verified by PCR technology genotype analysis²⁵ (details in supplement⁷). All mice were reared in a 12-hour:12-hour light:dark cycle. Mice of either sex, 1.5 to 2 months of age, were used for experimental procedures. All animals were treated according to the guidelines established by the Institute for Laboratory Animal Research (Guide for the Care and Use of Laboratory Animals), conformed to the Association for Research in Vision and Ophthalmology (ARVO) Statement for the Use of Animals in Ophthalmic and Vision Research, and were approved by the appropriate animal committees of USC and the Atlanta Veterans Administration Medical Center.

Optokinetic Tracking (OKT)

Mice were placed on a small platform in the center of four computer monitors that formed a virtual drum with a rotating vertical sine wave grating (12°/s [d/s]; OptoMotry; Cerebral Mechanics, Lethbridge, AB, Canada), as described previously.^{20,39} Reflexive head movements in the same direction as the rotating gratings were considered positive responses. Spatial frequency thresholds were determined with an increasing staircase paradigm starting at 0.042 cycles/deg (c/d) with 100% contrast. Contrast sensitivity thresholds were measured across five spatial frequencies (0.031, 0.064, 0.092, 0.103, and 0.192 c/d).⁴⁰

Electroretinography (ERG)

Photopic ERGs were performed as described previously.^{15,20} Each mouse was anesthetized and flash stimuli of 10 μs duration (from 0.2–20 Hz) was delivered to the eye of the mouse from which recordings were taken. For photopic cone readings, continuous white background light of 8 foot candles (fc; 200 cd-s/m²) was delivered to the recorded eye for 1 minute before the first flash was administered and light adaptation recordings began. Additional flash recordings were taken for 2 up to 15 minutes of light adaptation. Responses were taken every 2 minutes up to 15 minutes of light adaptation recorded from a flash, and the a-wave and b-wave amplitudes from the first flash were averaged and presented in Figure 1. The mice were fully light-adapted by 15 minutes, so the ERG amplitudes from the 15-minute time point are presented in Figure 1 (See representative traces in Supplementary Fig. S1). These amplitudes reflect the average of the recorded ERG amplitudes from 20 flashes at each frequency.

After the flash recordings had been taken, flicker responses were recorded. Averages from 10 to 20 sweeps were recorded and averaged for each data point. To determine the optimal flash intensity, 10 Hz flicker responses were recorded using

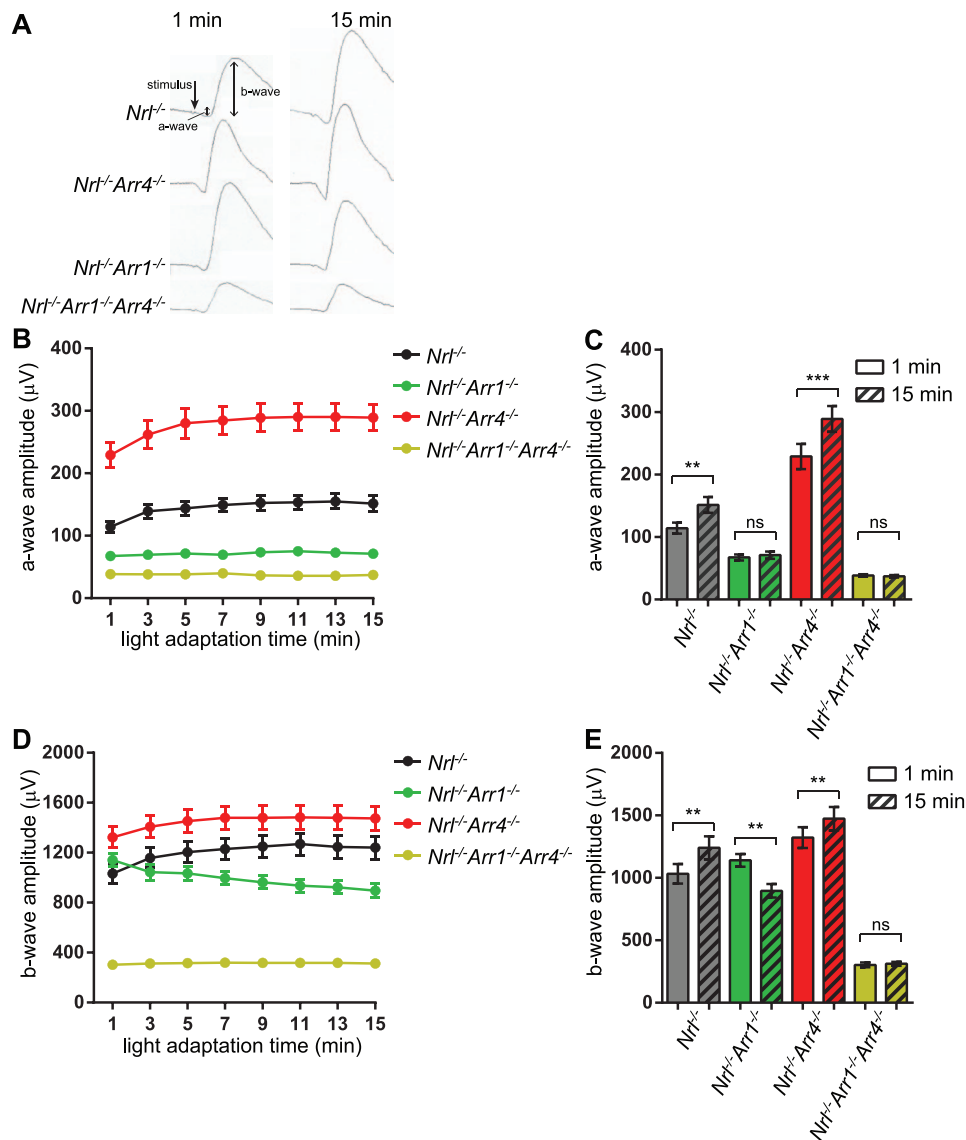


FIGURE 1. Light adaptation studies. (A) Representative waveforms of the photopic ERG response of each genotype at 1 minute after light exposure and after 15 minutes of light exposure. (B) Photopic ERG a-wave amplitudes beginning at 1 minute after light exposure and continuing through 15 minutes. (C) Light adaptation was measured by comparing the a-wave amplitudes after 1 and 15 minutes of light exposure by a Student's t-test. *Nrt*^{-/-} and *Nrt*^{-/-}*Arr4*^{-/-} mice displayed a significant increase in a-wave amplitudes (** $P = 0.0029$ and *** $P < 0.001$, respectively), while *Nrt*^{-/-}*Arr1*^{-/-} and *Nrt*^{-/-}*Arr1*^{-/-}*Arr4*^{-/-} did not increase between 1 and 15 minutes ($P = 0.5634$ and $P = 0.6406$, respectively). (D) Photopic ERG b-wave amplitudes from 1 to 15 minutes of light exposure. (E) Light adaptation was measured as in (C). *Nrt*^{-/-} and *Nrt*^{-/-}*Arr4*^{-/-} mice displayed a significant increase in b-wave amplitudes (** $P = 0.0032$ and ** $P = 0.0011$, respectively), while *Nrt*^{-/-}*Arr1*^{-/-} b-wave amplitudes decreased (** $P = 0.0067$) and *Nrt*^{-/-}*Arr1*^{-/-}*Arr4*^{-/-} did not change over time ($P = 0.6069$). ns, not significant.

flash intensities from -1.59 to 2.01 log cd-s/m². Further studies comparing ERG amplitudes across multiple flash frequencies, from 0.2 to 20 Hz, used a flash intensity of 2.01 log cd-s/m².

Immunoblot Analysis

Immunoblot analysis was performed as described previously.^{15,20,33} Briefly, after dissection, each mouse retina was flash frozen and homogenized in 50 mM Tris buffer with cComplete Protease Inhibitor Cocktail (Hoffman-La Roche, Basel, Switzerland). A total of 60 µg of protein per retina was resolved on replicate 10% SDS-PAGE (each lane containing a portion of total retinal homogenate from a different mouse), transferred to nitrocellulose membranes (Li-Cor, Lincoln, NE, USA), and incubated sequentially with antibodies for either S-opsin (1:5000) or M-opsin (1:5000),³³ followed by loading control,

β-actin (1:4000). Appropriate secondary antibodies conjugated to a fluorophore (600 or 800 nm) allowed detection using the Li-Cor Odyssey infrared detection system. Li-Cor Odyssey v. 3.1 was used to quantify the intensity of each band. Relative amounts of the opsins were calculated by dividing the intensity of the M- or S-opsin band by the intensity of the β-actin band. The average of the *Nrt*^{-/-} samples was set as 100%.⁷

Immunohistochemistry (IHC)

Immunohistochemistry was performed as described previously.^{20,41} Retinal sections were obtained from mouse eyes fixed in 4% paraformaldehyde in PBS for 1 hour on ice. Lenses were removed before the eyes were embedded in optimal cutting temperature (OCT) medium (Sakura Finetechnical, Torrance, CA, USA) and snap frozen in liquid nitrogen. Frozen retinal

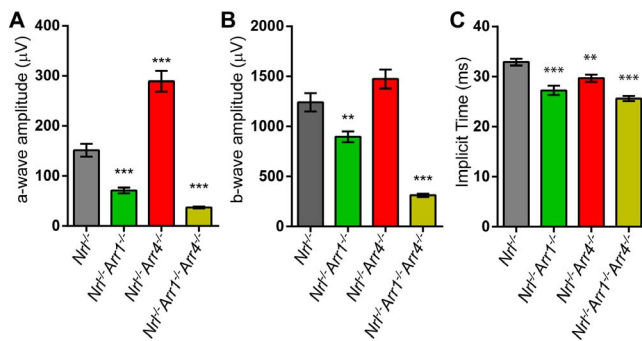


FIGURE 2. Photopic ERG results. (A) A-wave amplitudes of the *Nrt*^{-/-}, *Nrt*^{-/-}*Arr1*^{-/-}, *Nrt*^{-/-}*Arr4*^{-/-}, and *Nrt*^{-/-}*Arr1*^{-/-}*Arr4*^{-/-} genotypes. These are the same data displayed as the 15-minute amplitudes in Figures 1B and 1C. *Significant differences compared to *Nrt*^{-/-} mice, as determined by 1-way ANOVA with post hoc multiple comparisons. The photopic ERG a-wave amplitude of *Nrt*^{-/-}*Arr1*^{-/-} was 53% less than *Nrt*^{-/-} (****P* < 0.001), *Nrt*^{-/-}*Arr4*^{-/-} was 91% greater than *Nrt*^{-/-} (****P* < 0.001), and the a-wave amplitude of *Nrt*^{-/-}*Arr1*^{-/-}*Arr4*^{-/-} was 75% less than that of *Nrt*^{-/-} (****P* < 0.001). (B) B-wave amplitudes of all four mouse genotypes (same as 15-minute time point in Figures 1D and 1E). The b-wave amplitude of *Nrt*^{-/-}*Arr1*^{-/-} mice was decreased by 28% compared to *Nrt*^{-/-} (***P* < 0.01) and the *Nrt*^{-/-}*Arr1*^{-/-}*Arr4*^{-/-} mice had b-wave amplitudes that were 75% less than *Nrt*^{-/-} (****P* < 0.001). (C) Photopic ERG a-wave implicit times for all four genotypes. *Nrt*^{-/-} mice had slower implicit times compared to *Nrt*^{-/-}*Arr1*^{-/-} (****P* < 0.001), *Nrt*^{-/-}*Arr4*^{-/-} (***P* < 0.01), and *Nrt*^{-/-}*Arr1*^{-/-}*Arr4*^{-/-} (****P* < 0.001). Differences were determined using 1-way ANOVA with post hoc multiple comparisons.

sections were cut in a cryostat at 10 µm thickness along the vertical median through the optic nerve and were placed on SuperFrost Plus (VWR International, Radnor, PA, USA) glass slides. Sections were rehydrated in PBS and blocked with blocking buffer (10% ChemiBlocker; Millipore, Billerica, MA, USA) in PBS) for 30 minutes at room temperature, then incubated at 4°C overnight with affinity purified rabbit polyclonal antibodies for either mouse S-opsin or mouse M-opsin (dilution 1:1000).³⁵ Slides were incubated with appropriate Alexa-Fluor 488-conjugated secondary antibodies (1:500; Invitrogen, Carlsbad, CA, USA) for 1 hour at room temperature. The slides were mounted using hard-set mounting medium with 4',6-diamidino-2-phenylindole DAPI (Vectashield; Vector Laboratories, Burlingame, CA, USA) and covered with a glass coverslip.

Statistical Analysis

All statistical analyses were performed using GraphPad Prism 6 (La Jolla, CA, USA). For comparison of the four genotypes, 1-way ANOVA analysis was performed with post hoc Dunnett's multiple comparisons test to determine if each genotype was different from *Nrt*^{-/-}. For comparison of four genotypes across multiple times, flash frequencies, or flash intensities, 2-way ANOVA analysis was performed with two factors: genotype and either time, frequency, or intensity. To compare the means across all values of the second factor (e.g., all flash intensities from -1.59 to 2.01 log cd-s/m²), Bonferroni's multiple comparisons test was performed to determine whether the mean of each genotype was different from *Nrt*^{-/-}. To compare the means at specific values of the second factor (e.g., at each flash intensity separately), Dunnett's multiple comparisons test was performed.

All charts display the data as mean ± SEM. For analysis of light adaptation, paired *t*-tests were performed to determine whether the ERG amplitudes were significantly different

between 1 and 15 minutes of light exposure within each genotype.¹⁵

RESULTS

ARR1 is Essential for Normal Light Adaptation

We previously reported that *Arr1*^{-/-} and *Arr1*^{-/-}*Arr4*^{-/-} mice have defects with light adaptation, while *Arr4*^{-/-} light adapt normally.¹⁵ To determine if ARR1 also is necessary for light adaptation in an all-cone retina, light adaptation was measured using visual arrestin knockouts on an *Nrt*^{-/-} background (Fig. 1). *Nrt*^{-/-} mice light adapted normally, indicated by an increase in the ERG a-wave and b-wave amplitude between 1 minute of light adaptation and the amplitude after 15 minutes of light adaptation (Student's paired *t*-test, a-wave, *P* = 0.0029; b-wave, *P* = 0.0032). *Nrt*^{-/-}*Arr4*^{-/-} mice also displayed normal light adaptation (a-wave, *P* < 0.001; b-wave, *P* = 0.0011), but *Nrt*^{-/-}*Arr1*^{-/-} (a-wave, *P* = 0.53; b-wave, decreased, *P* = 0.0067) and *Nrt*^{-/-}*Arr1*^{-/-}*Arr4*^{-/-} (a-wave, *P* = 0.64; b-wave, *P* = 0.6069) do not light adapt. This indicated that expression of ARR1 is necessary and sufficient for normal light-adaptation, while ARR4 is not required.

ERG Amplitudes Are Increased in *Nrt*^{-/-}*Arr4*^{-/-} and Decreased in *Nrt*^{-/-}*Arr1*^{-/-} and *Nrt*^{-/-}*Arr1*^{-/-}*Arr4*^{-/-} Mice

To test the hypothesis that the cone-driven phenotypes of the *Nrt*^{-/-}, *Nrt*^{-/-}*Arr4*^{-/-}, and *Nrt*^{-/-}*Arr1*^{-/-} mice would be different from one another, and that the *Nrt*^{-/-}*Arr1*^{-/-}*Arr4*^{-/-} mice would display the most severe phenotype, the ERG amplitudes of light-adapted mice were compared. Electroretinographic recordings were done after 15 minutes of light adaptation (Figs. 2A, 2B). A 1-way ANOVA of the a-wave amplitudes, reflective of photoreceptor response, determined that there were significant differences between groups (*F*[3,51] = 7.239; *P* < 0.001). Post hoc multiple comparisons revealed that the *Nrt*^{-/-}*Arr4*^{-/-} a-wave amplitudes were, on average, 91% greater than the *Nrt*^{-/-} a-wave amplitudes (*P* < 0.001), while the other two groups, *Nrt*^{-/-}*Arr1*^{-/-} and *Nrt*^{-/-}*Arr1*^{-/-}*Arr4*^{-/-}, were significantly lower than *Nrt*^{-/-} 53% lower, *P* < 0.001 and 75% lower, *P* < 0.001, respectively; (Fig. 2A). It is noteworthy that the *Nrt*^{-/-}*Arr4*^{-/-} and *Nrt*^{-/-}*Arr1*^{-/-} mice have distinct phenotypes from *Nrt*^{-/-} and from one another, indicating separate functions for the two visual arrestins within the cones.

A 1-way ANOVA of the paired-flash b-wave amplitudes, reflective of ON bipolar cell function,⁴²⁻⁴⁴ also revealed significant differences between groups (*F*[3,51] = 43.74; *P* < 0.001). *Nrt*^{-/-}*Arr4*^{-/-} was slightly higher than *Nrt*^{-/-} (18% increase), but this difference did not reach statistical significance. *Nrt*^{-/-}*Arr1*^{-/-} and *Nrt*^{-/-}*Arr1*^{-/-}*Arr4*^{-/-} had decreased amplitudes compared to *Nrt*^{-/-} mice (28% reduction, *P* < 0.01 and 75% reduction, *P* < 0.001, respectively; Fig. 2B).

ERG Implicit Time is Decreased in All Visual Arrestin Knockout Genotypes

Another important feature of ERG recordings is the implicit time of the a-wave, which reflects the speed of the phototransduction cascade; smaller values (measured in ms) indicated a faster photoreceptor response to the light stimulus. We compared the a-wave implicit times between the four genotypes to determine if the absence of the visual arrestins would affect the timing of the photoreceptor response. This was indeed the case; after 15 minutes of light adaptation, the *Nrt*^{-/-} mice had a-wave implicit

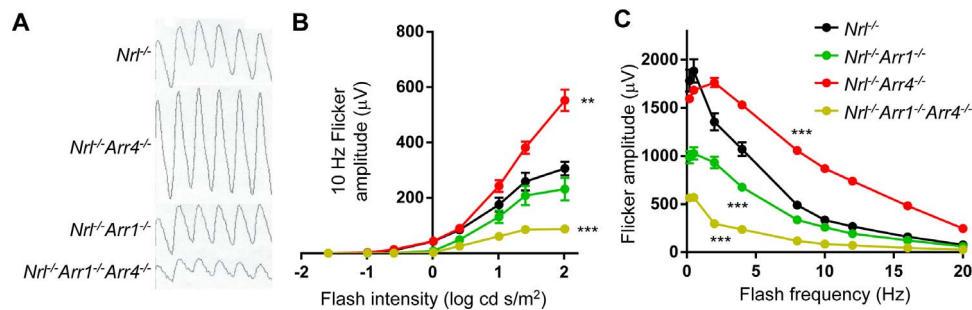


FIGURE 3. Photopic flicker ERG response results. (A) Representative flicker waveforms at 10 Hz in response to 2.01 log cd-s/m² stimuli for each of the four genotypes. (B) Flicker amplitudes at 10 Hz across multiple intensities, ranging from -1.59 to 2.01 log cd-s/m². *Significant difference compared to *Nrt*^{-/-} mice, as determined by 2-way ANOVA with post hoc multiple comparisons. *Nrt*^{-/-}*Arr4*^{-/-} was significantly increased compared to *Nrt*^{-/-} (** $P < 0.01$) and *Nrt*^{-/-}*Arr1*^{-/-}*Arr4*^{-/-} was significantly decreased compared to *Nrt*^{-/-} (*** $P < 0.001$). (C) Flicker amplitudes with a flash intensity of 2.01 log cd-s/m² across multiple frequencies, ranging from 0.2 to 20 Hz. All three arrestin knockout genotypes were significantly different from *Nrt*^{-/-} mice, with *Nrt*^{-/-}*Arr4*^{-/-} mice having larger amplitudes compared to *Nrt*^{-/-} (*** $P < 0.001$) and *Nrt*^{-/-}*Arr1*^{-/-} mice and *Nrt*^{-/-}*Arr1*^{-/-}*Arr4*^{-/-} mice having smaller amplitudes than *Nrt*^{-/-} mice (*** $P < 0.001$ for both).

times that were greater than all other groups (Fig. 2C; 1-way ANOVA, $F[3,51] = 20.49$; $P < 0.001$). Post hoc multiple comparisons revealed that *Nrt*^{-/-}*Arr1*^{-/-} (17% decrease, $P < 0.001$), *Nrt*^{-/-}*Arr4*^{-/-} (10% decrease, $P < 0.01$), and *Nrt*^{-/-}*Arr1*^{-/-}*Arr4*^{-/-} (32% decrease, $P < 0.001$) all had faster a-wave implicit times than *Nrt*^{-/-}.

ERG Flicker Amplitudes Reveal Distinct Phenotypes of *Nrt*^{-/-}*Arr4*^{-/-} and *Nrt*^{-/-}*Arr1*^{-/-}*Arr4*^{-/-}

To further probe cone electrophysiological pathways, mice were stimulated with flashes at 10 Hz across multiple intensities, ranging from -1.59 to 2.01 log cd-s/m² (Figs. 3A, 3B). The lower light intensities are similar to those used in human studies, while the brightest intensity has been used in previous studies of ARR1 and ARR4 function in wild-type mice.^{15,20} The flash stimulus did not have the same effect for all genotypes (2-way ANOVA, $F[21,161] = 21.49$; $P < 0.001$). The amplitudes of *Nrt*^{-/-}*Arr4*^{-/-} mice were significantly increased across flash stimuli (50%, $P < 0.01$) compared to *Nrt*^{-/-}. In contrast, *Nrt*^{-/-}*Arr1*^{-/-}*Arr4*^{-/-} mice had significantly lower (70% decrease, $P < 0.001$) amplitudes than *Nrt*^{-/-}. The response from *Nrt*^{-/-}*Arr1*^{-/-} mice was not significantly different from *Nrt*^{-/-} mice. These results were consistent with our flash recordings that showed that *Nrt*^{-/-}*Arr1*^{-/-} and *Nrt*^{-/-}*Arr4*^{-/-} mice had different phenotypes and that *Nrt*^{-/-}*Arr1*^{-/-}*Arr4*^{-/-} had the most severe phenotype. Although the difference is most obvious at the brightest light intensity, the pattern is consistent across all intensities measured.

Further ERG flicker response experiments were done to determine if this pattern was consistent across a range of flash frequencies. Using the brightest flash stimulus, 2.01 log cd-s/m², flicker response studies were performed at multiple flash frequencies, from 0.2 to 20 Hz (Fig. 3C). The genotypes had different responses to flash frequencies (2-way ANOVA, $F[24,200] = 57.73$; $P < 0.001$). *Nrt*^{-/-} mice were significantly different than all three other genotypes: *Nrt*^{-/-}*Arr1*^{-/-} (38% average reduction; $P < 0.001$), *Nrt*^{-/-}*Arr4*^{-/-} (34% average increase; $P < 0.001$), and *Nrt*^{-/-}*Arr1*^{-/-}*Arr4*^{-/-} (72% average reduction; $P < 0.001$). These differences are consistent with the more subtle, but nonsignificant, changes in the paired-flash b-wave amplitudes seen in Figure 2B. Figure 3C demonstrates that those differences were particularly large at frequencies below 10 Hz, and that *Nrt*^{-/-}*Arr1*^{-/-} and *Nrt*^{-/-}*Arr4*^{-/-} amplitudes were respectively smaller and larger than the

Nrt^{-/-} mice. This is consistent with our hypothesis that ARR1 and ARR4 do, indeed, perform independent functions in cones, because the phenotypes of their respective knockouts are opposite one another. In addition, when visual arrestins are not expressed in the cones, there was an even greater deficit, resulting in the large decrease in b-wave paired flash amplitudes (Fig. 2B) and multiflash amplitudes across many light intensities and flash frequencies (Figs. 3B, 3C).

M- and S-Opsin Expression Levels Are Altered in the Visual Arrestin Knockouts

The enhanced photopic ERG a-wave amplitudes observed in the *Nrt*^{-/-}*Arr4*^{-/-} mice are the result of an unknown mechanism. Previous work showed that M-opsin expression was greater in the inferior retina in *Arr4*^{-/-} compared to WT mice,²⁰ and we hypothesized that this increase in M-opsin expression contributed to the enhanced photopic ERG b-wave amplitudes observed in *Arr4*^{-/-} mice. To determine whether cone opsin expression correlates with the observed photopic ERG amplitudes in the all-cone retina, immunoblot analysis was performed on total retinal homogenates to quantitatively determine the relative total amounts of M- and S-opsin in each mouse genotype (Fig. 4). There were significant differences between genotypes (1-way ANOVA, $F[3,8] = 69.05$; $P < 0.001$). Surprisingly, there was no difference in M-opsin protein immunoreactivity between *Nrt*^{-/-} and *Nrt*^{-/-}*Arr4*^{-/-} mice. *Nrt*^{-/-}*Arr1*^{-/-} (58% decrease, $P < 0.001$) and *Nrt*^{-/-}*Arr1*^{-/-}*Arr4*^{-/-} (54% decrease, $P < 0.001$) had a significant decrease in M-opsin compared to *Nrt*^{-/-} (Figs. 4A, 4B). These decreases correlate with the lower photopic ERG amplitudes for genotypes.

Differences between genotypes in S-opsin expression level also were observed (1-way ANOVA, $F[3,8] = 41.14$, $P < 0.001$) (Figs. 4C, 4D). Compared to *Nrt*^{-/-}, *Nrt*^{-/-}*Arr1*^{-/-} retinas had an increase in S-opsin immunoreactive protein (21% increase, $P < 0.05$). *Nrt*^{-/-}*Arr4*^{-/-} and *Nrt*^{-/-}*Arr1*^{-/-}*Arr4*^{-/-} mouse retinas had less S-opsin expression than *Nrt*^{-/-} (51% decrease, $P < 0.001$ and 31% decrease, $P < 0.01$, respectively).

M-Opsin Expression Is Not Confined to Cone Outer Segments for All Four Genotypes

A previous study showed that M-opsin is not confined to the cone photoreceptor outer segments in *Nrt*^{-/-} mice but was instead present throughout the cone cell bodies, while S-opsin is only in the cone outer segments in *Nrt*^{-/-} mice.⁴⁵ It also has been demonstrated that the cone outer segments are

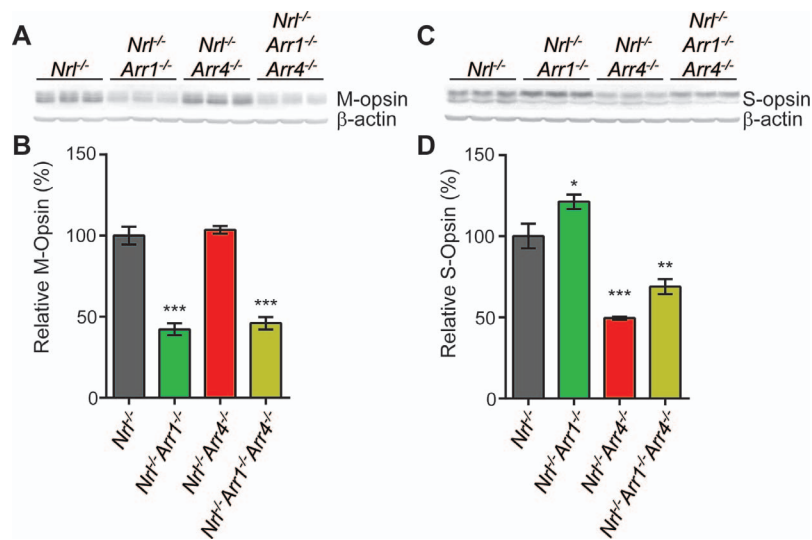


FIGURE 4. Immunoblot analysis of M- and S-opsins using total retinal homogenates. (A) Image of the immunoblot using anti-M-opsin primary antibody and anti- β -actin primary antibody as a loading control. Each lane contains an aliquot from total retinal homogenate from a different mouse (3 mice per genotype). (B) Quantitative analysis of the relative amount of M-opsin in the blot pictured in (A). The ratio of the intensity of the M-opsin band compared to the intensity of the corresponding β -actin band was calculated for each lane, and the mean and SEM was calculated for each genotype. The mean of the *Nrt*^{-/-} lanes was set as 100%. *Nrt*^{-/-}*Arr1*^{-/-} (***) ($P < 0.001$) and *Nrt*^{-/-}*Arr1*^{-/-}*Arr4*^{-/-} (***) ($P < 0.001$) had significantly less immunoreactive M-opsin than *Nrt*^{-/-} mice. There was no difference between *Nrt*^{-/-} and *Nrt*^{-/-}*Arr4*^{-/-} mice. (C) Image of the immunoblot using anti-S-opsin primary antibody and anti- β -actin primary antibody as a loading control. (D) Relative S-opsin was calculated as for M-opsin above. *Nrt*^{-/-}*Arr1*^{-/-} mice expressed more immunoreactive S-opsin than *Nrt*^{-/-} (* $P < 0.05$), while *Nrt*^{-/-}*Arr4*^{-/-} (***) ($P < 0.001$) and *Nrt*^{-/-}*Arr1*^{-/-}*Arr4*^{-/-} mice (** $P < 0.01$) expressed less S-opsin.

decreased in length in *Nrt*^{-/-} mice compared to WT.^{25,46} To determine if the visual arrestins impact the subcellular localization of the cone opsins, IHC analysis was performed using frozen vertical retina sections from each genotype. Primary specific antibodies that were developed against unique amino terminal peptides in mouse M-opsin and S-opsin,³³ followed by fluorescent secondary antibodies, were used to determine the location of M- and S-opsin expression in the photoreceptors. M-opsin was not confined to the outer segments of the cones for all genotypes, and a significant amount of M-opsin was observed in the cell bodies, axons, and axon terminals of the M-opsin expressing cones (Fig. 5). Interestingly, S-opsin was confined completely to the cone outer segments for all genotypes (Fig. 5). M- and S-opsin immunological reactive staining of the cone outer segments confirmed that the absence of the visual arrestins did not increase the length of the outer segments in the *Nrt*^{-/-} mice.

Contrast Sensitivity and Visual Acuity Are Impacted by the Lack of Visual Arrestins

Previous results revealed that the *Arr4*^{-/-} mouse displayed significantly decreased contrast sensitivity and visual acuity thresholds compared to WT.²⁰ Based on these findings, we expected to observe similar, if not enhanced, OKT behavioral phenotypes in the all-cone *Nrt*^{-/-} and *Nrt*^{-/-}*Arr4*^{-/-} mice. Surprisingly, there was no significant decrease in visual acuity in *Nrt*^{-/-}*Arr4*^{-/-} or *Nrt*^{-/-}*Arr1*^{-/-} compared to *Nrt*^{-/-}, but there was a 30% decrease in visual acuity threshold for *Nrt*^{-/-}*Arr1*^{-/-}*Arr4*^{-/-} mice (Fig. 6A; 1-way ANOVA, $F[3,17] = 37.16$; $P < 0.001$).

Furthermore, loss of visual arrestins significantly altered the contrast sensitivity curves (2-way ANOVA, $F[12,68] = 12.87$; $P < 0.001$). At the peak spatial frequency of 0.092 c/d, *Nrt*^{-/-}*Arr4*^{-/-} and *Nrt*^{-/-}*Arr1*^{-/-}*Arr4*^{-/-} had significantly

lower contrast sensitivity (16% decrease, $P < 0.001$ and 25% decrease, $P < 0.001$, respectively) compared to *Nrt*^{-/-} mice. *Nrt*^{-/-}*Arr1*^{-/-} mice displayed an opposite response with higher contrast sensitivity (16% increase, $P < 0.01$) than *Nrt*^{-/-} mice. These results indicated that ARR4 is more critical for maintaining normal contrast sensitivity than ARR1.

DISCUSSION

In this study, we tested the hypotheses that *Nrt*^{-/-}*Arr1*^{-/-} and *Nrt*^{-/-}*Arr4*^{-/-} mice would display distinct visual phenotypes compared to *Nrt*^{-/-} mice and compared to each other. We proposed that these differences are due to the unique and nonoverlapping functions of the two visual arrestins within the photoreceptors, aside from their shared ability to shut off cone phototransduction by binding the light-activated, GRK1 phosphorylated cone opsins.^{33,46,47} We further hypothesized that the *Nrt*^{-/-}*Arr1*^{-/-}*Arr4*^{-/-} mice would have the most severe visual phenotypes, because when mice lack both visual arrestins, they display defective cone phototransduction shutoff.⁷

Phototransduction Shutoff Versus Other Functions in the Cones

Consistent with our hypothesis, in all ERG experiments the *Nrt*^{-/-}*Arr1*^{-/-}*Arr4*^{-/-} mice displayed the most severe visual phenotype. They displayed significantly decreased photopic ERG a-wave, b-wave, and flicker amplitude responses compared to *Nrt*^{-/-} mice. In addition, they do not light adapt, and have the fastest implicit time of all of the genotypes. In our optokinetic tracking studies, *Nrt*^{-/-}*Arr1*^{-/-}*Arr4*^{-/-} was the only genotype with a decrease in visual acuity compared to *Nrt*^{-/-} mice, and *Nrt*^{-/-}*Arr1*^{-/-}*Arr4*^{-/-} mice have the lowest contrast sensitivity of all genotypes. The ERG phenotypes are consistent with the

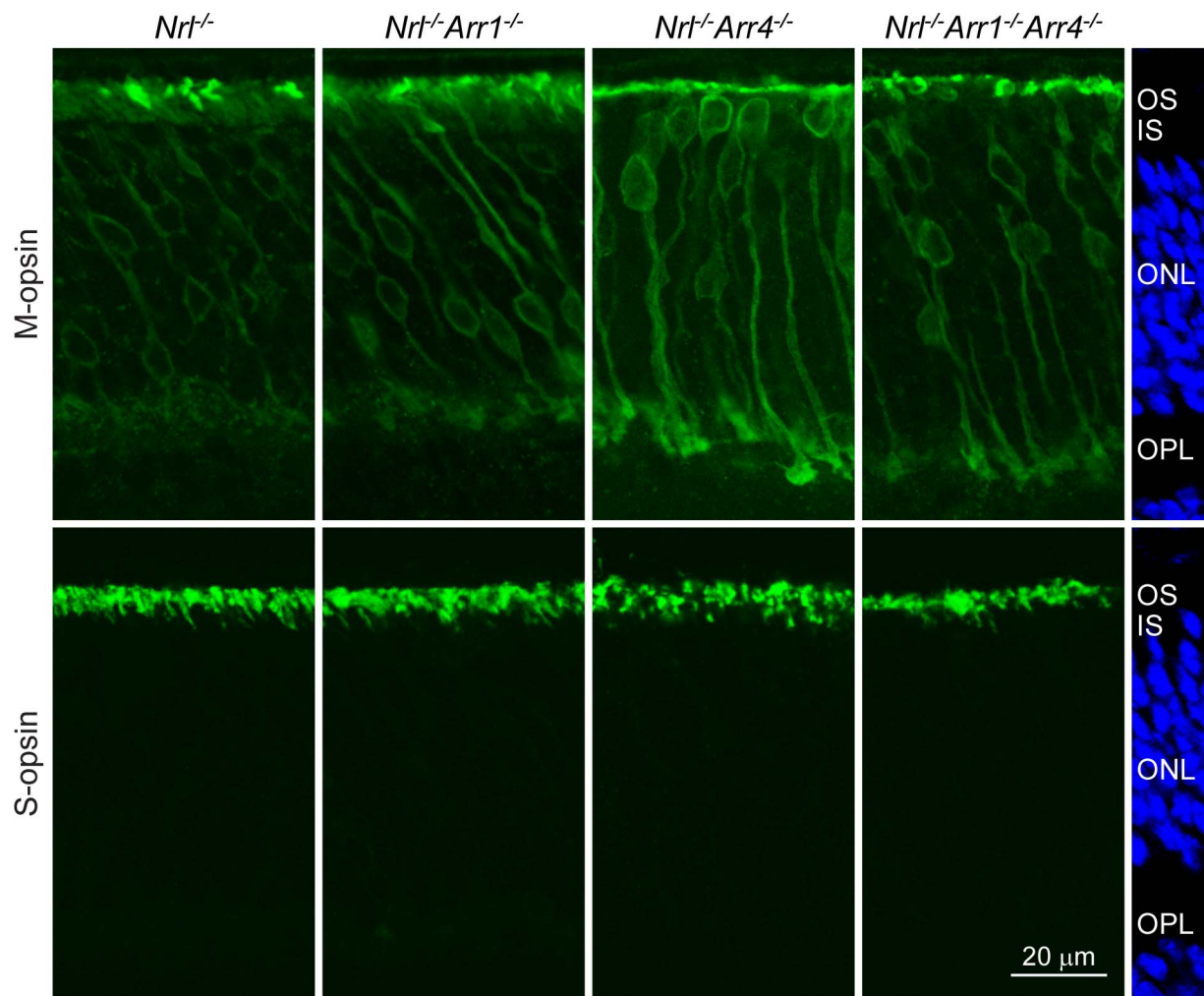


FIGURE 5. Immunohistochemical analysis of M- and S-opsin in visual arrestin knock-out mice on an all cone *Nrt*^{-/-} background. *Top row:* Sections were labeled with a primary antibody raised against M-opsin followed by a fluorescent secondary antibody (green). All genotypes displayed a mislocalization of M-opsin in the cone cell bodies, axons, and axon terminals. *Bottom row:* Sections were labeled with a primary antibody raised against S-opsin followed by a fluorescent secondary antibody (green). S-opsin was confined to the cone outer segments for all genotypes. The images on the right display DAPI stain for retina location reference. ONL, outer nuclear layer; OPL, outer plexiform layer. Scale bar: 20 µm.

phenotypes observed for WT and *Arr1*^{-/-}*Arr4*^{-/-} mice,^{15,20} indicating that the all-cone retina of the *Nrt*^{-/-} mouse did not have a significant impact on the overall phenotypes of mice with or without visual arrestins. We propose that these phenotypes are due to the defect in cone phototransduction shutoff that results from the absence of ARR1 and ARR4. In these mice, the opsins are not bound by arrestins and the phototransduction cascade is not properly turned off.

The differences between *Nrt*^{-/-}, *Nrt*^{-/-}*Arr1*^{-/-}, and *Nrt*^{-/-}*Arr4*^{-/-} mice likely have less to do with phototransduction shutoff, because based on single-cell recordings, phototransduction shutoff occurs normally as long as one visual arrestin is present.⁷ We hypothesized that the phenotypes of the *Nrt*^{-/-}*Arr1*^{-/-} and *Nrt*^{-/-}*Arr4*^{-/-} mice would differ from one another and reflect the other, nonopsin-shutoff functions that the visual arrestins perform in cone photoreceptors. Surprisingly, *Nrt*^{-/-}*Arr1*^{-/-} and *Nrt*^{-/-}*Arr4*^{-/-} mice displayed opposite phenotypes in nearly all of our experimental results, including light adaptation, ERG amplitudes, and S- and M-opsin expression levels compared to *Nrt*^{-/-}.

Alternative, nonopsin shutoff-related functions of ARR1 and ARR4 have not been well characterized, although ARR1

has been shown to interact with and modulate other proteins in mammalian rods, including itself (homo-dimers and tetramers),^{1,48-50} microtubules,⁵¹⁻⁵³ Ca²⁺-bound calmodulin,⁵⁴ N-ethylmaleimide sensitive factor (NSF),¹⁷ MAP kinases JNK3⁵⁵ and ERK2,^{53,56,57} E3 ubiquitin ligase Mdm2,^{53,55} enolase,⁵⁸ Parkin,⁵⁹ and Bardet-Biedl syndrome 5 (BBS5).⁶⁰ The homo-oligomerization of ARR1 is thought to be a storage form that decreases the concentration of monomeric ARR1 (reviewed previously⁶¹), which is the only form that can bind light activated, phosphorylated rhodopsin.⁶² In addition, ARR1 binds microtubules and potentially keeps ARR1 confined to rod cell bodies and inner segments in the dark-adapted state,⁵⁰⁻⁵² and ARR1 modulates synaptic transmission and exocytosis through its interaction with NSF.¹⁷ In many of the studies, the physiological consequences of ARR1 binding and interacting with the other proteins listed above are unclear. A much smaller list of binding partners of ARR4 have been discovered, including JNK3 and MDM2,⁵⁵ RND2,⁶³ ALS2CR4/TMEM 237,⁶⁴ and DRD4.⁶⁵ We predict that more interacting partners of ARR4 will be uncovered with further study.

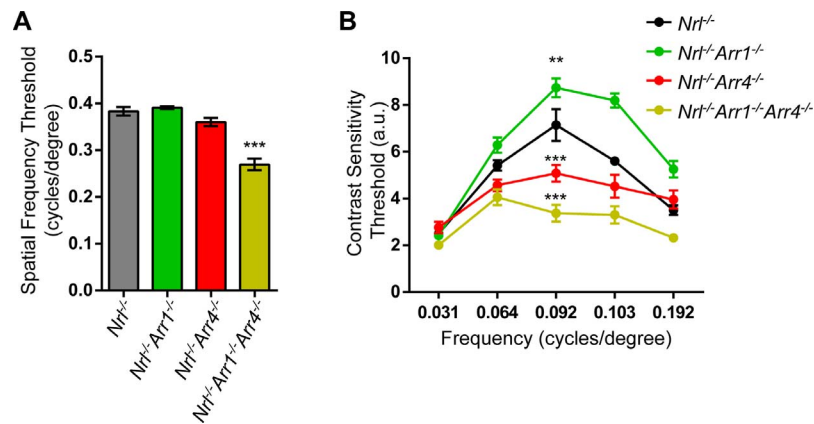


FIGURE 6. Visual function testing of visual arrestin mutants using optokinetic tracking (OKT). (A) Spatial frequency thresholds, indicating visual acuity of the mice. Only *Nrl*^{-/-}*Arr1*^{-/-}*Arr4*^{-/-} mice had a decreased spatial frequency threshold compared to *Nrl*^{-/-} (***P* < 0.001). (B) Contrast sensitivity of each mouse genotype, measured at frequencies from 0.031 to 0.192 c/d. At the peak of the contrast sensitivity (0.092 c/d), *Nrl*^{-/-}*Arr1*^{-/-} mice had a higher contrast sensitivity measurement than *Nrl*^{-/-} mice (***P* < 0.01), while *Nrl*^{-/-}*Arr4*^{-/-} (***P* < 0.001) and *Nrl*^{-/-}*Arr1*^{-/-}*Arr4*^{-/-} mice (***P* < 0.001) had significantly decreased contrast sensitivity compared to *Nrl*^{-/-} mice.

In contrast to the visual arrestins, the β -arrestins are known to have many alternative, non-GPCR shutoff functions and has been the subject of extensive study (reviewed previously^{66–68}). A recent in vitro study has demonstrated that the visual arrestins participate synergistically in the desensitization and internalization of a non-opsin GPCR, dopamine receptor D4 (DRD4).⁶⁵ This interaction may have a role in the circadian regulation of the expression of DRD4, which is involved in the regulation of cAMP and gap junctional coupling between photoreceptors. Based on the sequence and structural similarity of the visual and β -arrestins, as well as the high concentration of the visual arrestins in the photoreceptors, it is reasonable to expect that the visual arrestins also may be involved in some of these alternative functions in rod and cone photoreceptors, including roles in vesicular trafficking, nuclear transport, ubiquitination, and gene regulation.

Visual Arrestins and the Expression of M- and S-Opsin

We hypothesize that the photopic ERG and cone opsin expression phenotypes observed in the *Nrl*^{-/-}*Arr1*^{-/-} and *Nrl*^{-/-}*Arr4*^{-/-} mice are due to these alternative functions of the visual arrestins, but it will require further study to determine the exact molecular mechanisms causing the phenotypes. Previous work observed an increase in M-opsin expression in *Arr4*^{-/-} mice that may contribute to the enhanced photopic ERG phenotype.²⁰ This is consistent with previous research, which showed that scotopic ERG amplitudes correspond with rhodopsin expression^{69,70} and single-cell responses from cones correspond with the relative amounts of cone opsin expression.^{71,72}

In this study, no increased M-opsin immunoreactivity increase was noted in 2-month-old retinas with our immunoblot experiments (Fig. 4), and these data are consistent with our previous results in WT and *Arr4*^{-/-} mice.²⁰ However, *Arr4*^{-/-} mice displayed an increase in M-opsin expression in the inferior region of the retina using measurements of the immunofluorescent intensity, which was undetectable in the immunoblot analysis because it is a measure of the total retinal protein. Because a greater amount of M-opsin is observed in the superior region of the retina, this may have overshadowed the relative differences in the immunoblot analysis.

In the current study, we observed a slight increase in the M-opsin immunofluorescence intensity in the *Nrl*^{-/-}*Arr4*^{-/-} mice compared to the other groups and a notable variability in M-opsin expression that may be related to age. We were unable to quantitatively measure this result because of the whorls and rosettes present in the *Nrl*^{-/-} and *Nrl*^{-/-}*Arr4*^{-/-} retinas, which made the retinal immunological staining inconsistent and difficult to measure. However, it is likely that the increase in M-opsin expression in the inferior region of *Arr4*^{-/-} mouse retinas compared to WT also would occur in *Nrl*^{-/-}*Arr4*^{-/-} mice compared to *Nrl*^{-/-}, and that this contributes to the observed significant increase in ERG amplitudes. In addition, the *Nrl*^{-/-}*Arr1*^{-/-} and *Nrl*^{-/-}*Arr1*^{-/-}*Arr4*^{-/-} mice have a decrease in M-opsin immunoreactivity in the immunoblot experiments, and this is consistent with the decreased ERG amplitudes in these animals.

Interestingly, S-opsin is expressed at different levels across the four genotypes as well. *Nrl*^{-/-}*Arr1*^{-/-} mice have a slightly higher S-opsin expression level compared to *Nrl*^{-/-}, while S-opsin is decreased significantly in the *Nrl*^{-/-}*Arr4*^{-/-} and *Nrl*^{-/-}*Arr1*^{-/-}*Arr4*^{-/-} mice. Because *Nrl*^{-/-} mice express approximately 25- to 30-fold more S-opsin than WT while M-opsin expression is unchanged (data not shown), it might be expected that the amount of S-opsin expression would contribute more to the photopic ERG amplitudes than the M-opsin expression, which is approximately the same between WT and *Nrl*^{-/-} mice.²⁵ However, the photopic ERG stimulus range used in these experiments was from a Xenon flash bulb with peak intensities measured at 485, 530, and 543 nm (data not shown). These wavelengths are better able to stimulate M-opsin, which has a peak absorbance at 508 nm, than S-opsin, which has a peak absorbance around 360 nm.⁷³ Therefore, the stimulation of the M-cones is likely to have a much greater impact on the photopic ERG amplitudes than that of the S-cones, even though there are a greater number of S-cones in the *Nrl*^{-/-} retina.

Based on the differential expression of S-opsin and M-opsin across the genotypes lacking each visual arrestin, ARR1 and ARR4 may be involved in the developmental regulation, synthesis, turnover, or degradation of one or both cone opsins. Future studies will investigate the potential transcriptional regulation of these genes to experimentally determine if ARR1 and/or ARR4 interact with any transcription factors known to regulate M-opsin or S-opsin expression levels,^{74,75} including NRL.^{25,46} It also is feasible that ARR1 may have a chaperone

function, allowing it to prevent or slow the turnover and/or degradation of M-opsin and ARR4 mirrors this function for S-opsin, and without the visual arrestins the respective opsins are degraded at an increased rate.

In conclusion, the current study focused on the visual phenotypes without either or both visual arrestin genes being expressed in an all-cone retina and revealed that ARR1 and ARR4 perform shared and unique modulatory roles in cone photoreceptors that result in distinct visual phenotypes.

Acknowledgments

The authors thank Mary D. Allen (1911–2011) for her lifetime support of Doheny Eye Institute and our vision research program, as well as members and USC undergraduate students in our Mary D. Allen Laboratory for Vision Research for their technical contributions, including Lawrence Rife for excellent technical assistance in ERG recordings, Ernesto Barron for his assistance with confocal image training, and Ruqayyah Malik and Andrew Vargus for their assistance in preparing final figures.

Supported by Doheny Eye Institute's Inaugural Mary D. Allen Endowed Chair in Vision Research (CMC), and in part by grant awards from the National Institutes of Health-NEI R01-EY015851 (CMC), R01-EY016435 (MTP), EY03040 (Doheny Eye Institute, NEI Core Grant), Department of Veterans Affairs (MTP) and Research to Prevent Blindness (USC Ophthalmology), and the Mary D. Allen Foundation (CMC, JDD, JSP), Dorie Miller (JDD, JSP), William Hansen Sandberg Memorial Foundation (JDD, JSP), and Tony Gray Foundation (JDD).

Disclosure: **J.D. Deming**, None; **J.S. Pak**, None; **J. Shin**, None; **B.M. Brown**, None; **M.K. Kim**, None; **M.H. Aung**, None; **E.-J. Lee**, None; **M.T. Pardue**, None; **C.M. Craft**, None

References

- Wacker WB, Donoso LA, Kalsow CM, Yankeelov JA Jr, Organisciak DT. Experimental allergic uveitis. Isolation, characterization, and localization of a soluble uveitopathogenic antigen from bovine retina. *J Immunol*. 1977;119:1949–1958.
- Kuhn H, Hall SW, Wilden U. Light-induced binding of 48-kDa protein to photoreceptor membranes is highly enhanced by phosphorylation of rhodopsin. *FEBS Lett*. 1984;176:473–478.
- Pfister C, Chabre M, Plouet J, et al. Retinal S antigen identified as the 48K protein regulating light-dependent phosphodiesterase in rods. *Science*. 1985;228:891–893.
- Shinohara T, Donoso L, Wistow G, Dietzschold B, Craft C, Tao R. The structure of bovine retinal S-antigen: sequence analysis and identification of monoclonal antibody epitopes and uveitogenic site. *Jpn J Ophthalmol*. 1987;31:197–206.
- Nir I, Ransom N. S-antigen in rods and cones of the primate retina: different labeling patterns are revealed with antibodies directed against specific domains in the molecule. *J Histochem Cytochem*. 1992;40:343–352.
- Craft CM, Whitmore DH, Donoso LA. Differential expression of mRNA and protein encoding retinal and pineal S-antigen during the light/dark cycle. *J Neurochem*. 1990;55:1461–1473.
- Nikonov SS, Brown BM, Davis JA, et al. Mouse cones require an arrestin for normal inactivation of phototransduction. *Neuron*. 2008;59:462–474.
- Craft CM, Whitmore DH, Wiechmann AF. Cone arrestin identified by targeting expression of a functional family. *J Biol Chem*. 1994;269:4613–4619.
- Miller JL, Fox DA, Litman BJ. Amplification of phosphodiesterase activation is greatly reduced by rhodopsin phosphorylation. *Biochemistry*. 1986;25:4983–4988.
- Wilden U, Hall SW, Kuhn H. Phosphodiesterase activation by photoexcited rhodopsin is quenched when rhodopsin is phosphorylated and binds the intrinsic 48-kDa protein of rod outer segments. *Proc Natl Acad Sci U S A*. 1986;83:1174–1178.
- Kuhn H. Light-regulated binding of rhodopsin kinase and other proteins to cattle photoreceptor membranes. *Biochemistry*. 1978;17:4389–4395.
- Xu J, Dodd RL, Makino CL, Simon MI, Baylor DA, Chen J. Prolonged photoresponses in transgenic mouse rods lacking arrestin. *Nature*. 1997;389:505–509.
- Mendez A, Burns ME, Roca A, et al. Rapid and reproducible deactivation of rhodopsin requires multiple phosphorylation sites. *Neuron*. 2000;28:153–164.
- Chen J, Simon MI, Matthes MT, Yasumura D, LaVail MM. Increased susceptibility to light damage in an arrestin knockout mouse model of Oguchi disease (stationary night blindness). *Invest Ophthalmol Vis Sci*. 1999;40:2978–2982.
- Brown BM, Ramirez T, Rife L, Craft CM. Visual Arrestin 1 contributes to cone photoreceptor survival and light adaptation. *Invest Ophthalmol Vis Sci*. 2010;51:2372–2380.
- Chan S, Rubin WW, Mendez A, et al. Functional comparisons of visual arrestins in rod photoreceptors of transgenic mice. *Invest Ophthalmol Vis Sci*. 2007;48:1968–1975.
- Huang SP, Brown BM, Craft CM. Visual Arrestin 1 acts as a modulator for N-ethylmaleimide-sensitive factor in the photoreceptor synapse. *J Neurosci*. 2010;30:9381–9391.
- Craft CM, Whitmore DH. The arrestin superfamily: cone arrestins are a fourth family. *FEBS Lett*. 1995;362:247–255.
- Gurevich VV, Gurevich EV. The structural basis of arrestin-mediated regulation of G-protein-coupled receptors. *Pharmacol Ther*. 2006;110:465–502.
- Deming JD, Pak JS, Brown BM, et al. Visual cone Arrestin 4 contributes to visual function and cone health. *Invest Ophthalmol Vis Sci*. 2015;56:5407–5416.
- Renninger SL, Gesemann M, Neuhauss SC. Cone arrestin confers cone vision of high temporal resolution in zebrafish larvae. *Eur J Neurosci*. 2011;33:658–667.
- Swaroop A, Xu JZ, Pawar H, Jackson A, Skolnick C, Agarwal N. A conserved retina-specific gene encodes a basic motif/leucine zipper domain. *Proc Natl Acad Sci U S A*. 1992;89:266–270.
- Kumar R, Chen S, Scheurer D, et al. The bZIP transcription factor Nrl stimulates rhodopsin promoter activity in primary retinal cell cultures. *J Biol Chem*. 1996;271:29612–29618.
- Rehemtulla A, Warwar R, Kumar R, Ji X, Zack DJ, Swaroop A. The basic motif-leucine zipper transcription factor Nrl can positively regulate rhodopsin gene expression. *Proc Natl Acad Sci U S A*. 1996;93:191–195.
- Mears AJ, Kondo M, Swain PK, et al. Nrl is required for rod photoreceptor development. *Nat Genet*. 2001;29:447–452.
- Bessant DA, Payne AM, Mitton KP, et al. A mutation in NRL is associated with autosomal dominant retinitis pigmentosa. *Nat Genet*. 1999;21:355–356.
- Martinez-Gimeno M, Maseras M, Baiget M, et al. Mutations P51U and G122E in retinal transcription factor NRL associated with autosomal dominant and sporadic retinitis pigmentosa. *Hum Mutat*. 2001;17:520.
- Raven MA, Oh EC, Swaroop A, Reese BE. Afferent control of horizontal cell morphology revealed by genetic respecification of rods and cones. *J Neurosci*. 2007;27:3540–3547.
- Yetemian RM, Brown BM, Craft CM. Neovascularization, enhanced inflammatory response, and age-related cone dystrophy in the Nrl-/-Grk1-/- mouse retina. *Invest Ophthalmol Vis Sci*. 2010;51:6196–6206.

30. Hao H, Veleri S, Sun B, et al. Regulation of a novel isoform of receptor expression enhancing protein REEP6 in rod photoreceptors by bZIP transcription factor NRL. *Hum Mol Genet.* 2014;23:4260–4271.
31. Conley SM, al-Ubaidi MR, Han Z, Naash MI. Rim formation is not a prerequisite for distribution of cone photoreceptor outer segment proteins. *FASEB J.* 2014;28:3468–3479.
32. Ding XQ, Matveev A, Singh A, Komori N, Matsumoto H. Exploration of cone cyclic nucleotide-gated channel-interacting proteins using affinity purification and mass spectrometry. *Adv Exp Med Biol.* 2014;801:57–65.
33. Zhu X, Brown B, Li A, Mears AJ, Swaroop A, Craft CM. GRK1-dependent phosphorylation of S and M opsins and their binding to cone arrestin during cone phototransduction in the mouse retina. *J Neurosci.* 2003;23:6152–6160.
34. Dang L, Pulukuri S, Mears AJ, Swaroop A, Reese BE, Sitaramayya A. Connexin 36 in photoreceptor cells: studies on transgenic rod-less and cone-less mouse retinas. *Mol Vis.* 2004;10:323–327.
35. Nikonov SS, Daniele LL, Zhu X, Craft CM, Swaroop A, Pugh EN Jr. Photoreceptors of Nrl^{-/-} mice coexpress functional S- and M-cone opsins having distinct inactivation mechanisms. *J Gen Physiol.* 2005;125:287–304.
36. Ma H, Thapa A, Morris LM, et al. Loss of cone cyclic nucleotide-gated channel leads to alterations in light response modulating system and cellular stress response pathways: a gene expression profiling study. *Hum Mol Genet.* 2013;22:3906–3919.
37. Rajala A, Dighe R, Agbaga MP, Anderson RE, Rajala RV. Insulin receptor signaling in cones. *J Biol Chem.* 2013;288:19503–19515.
38. Xu J, Morris L, Thapa A, et al. cGMP accumulation causes photoreceptor degeneration in CNG channel deficiency: evidence of cGMP cytotoxicity independently of enhanced CNG channel function. *J Neurosci.* 2013;33:14939–14948.
39. Aung MH, Kim MK, Olson DE, Thule PM, Pardue MT. Early visual deficits in streptozotocin-induced diabetic long evans rats. *Invest Ophthalmol Vis Sci.* 2013;54:1370–1377.
40. Prusky GT, Alam NM, Beekman S, Douglas RM. Rapid quantification of adult and developing mouse spatial vision using a virtual optomotor system. *Invest Ophthalmol Vis Sci.* 2004;45:4611–4616.
41. Zhu X, Li A, Brown B, Weiss ER, Osawa S, Craft CM. Mouse cone arrestin expression pattern: light induced translocation in cone photoreceptors. *Mol Vis.* 2002;8:462–471.
42. Stockton RA, Slaughter MM. B-wave of the electroretinogram. A reflection of ON bipolar cell activity. *J Gen Physiol.* 1989;93:101–122.
43. Tian N, Slaughter MM. Correlation of dynamic responses in the ON bipolar neuron and the b-wave of the electroretinogram. *Vision Res.* 1995;35:1359–1364.
44. Abd-El-Barr MM, Pennesi ME, Saszik SM, et al. Genetic dissection of rod and cone pathways in the dark-adapted mouse retina. *J Neurophysiol.* 2009;102:1945–1955.
45. Roger JE, Ranganath K, Zhao L, et al. Preservation of cone photoreceptors after a rapid yet transient degeneration and remodeling in cone-only Nrl^{G \hat{A} E}/G \hat{A} E mouse retina. *J Neurosci.* 2012;32:528–541.
46. Daniele LL, Lillo C, Lyubarsky AL, et al. Cone-like morphological, molecular, and electrophysiological features of the photoreceptors of the Nrl knockout mouse. *Invest Ophthalmol Vis Sci.* 2005;46:2156–2167.
47. Sutton RB, Vishnivetskiy SA, Robert J, et al. Crystal structure of cone arrestin at 2.3Å: evolution of receptor specificity. *J Mol Biol.* 2005;354:1069–1080.
48. Imamoto Y, Tamura C, Kamikubo H, Kataoka M. Concentration-dependent tetramerization of bovine visual arrestin. *Biophys J.* 2003;85:1186–1195.
49. Schubert C, Hirsch JA, Gurevich VV, Engelman DM, Sigler PB, Fleming KG. Visual arrestin activity may be regulated by self-association. *J Biol Chem.* 1999;274:21186–21190.
50. Hanson SM, Van EN, Francis DJ, et al. Structure and function of the visual arrestin oligomer. *EMBO J.* 2007;26:1726–1736.
51. Nair KS, Hanson SM, Kennedy MJ, Hurley JB, Gurevich VV, Slepak VZ. Direct binding of visual arrestin to microtubules determines the differential subcellular localization of its splice variants in rod photoreceptors. *J Biol Chem.* 2004;279:41240–41248.
52. Hanson SM, Francis DJ, Vishnivetskiy SA, Klug CS, Gurevich VV. Visual arrestin binding to microtubules involves a distinct conformational change. *J Biol Chem.* 2006;281:9765–9772.
53. Hanson SM, Cleghorn WM, Francis DJ, et al. Arrestin mobilizes signaling proteins to the cytoskeleton and redirects their activity. *J Mol Biol.* 2007;368:375–387.
54. Wu N, Hanson SM, Francis DJ, et al. Arrestin binding to calmodulin: a direct interaction between two ubiquitous signaling proteins. *J Mol Biol.* 2006;364:955–963.
55. Song X, Raman D, Gurevich EV, Vishnivetskiy SA, Gurevich VV. Visual and non-visual arrestins in their “inactive” conformation bind JNK3 and Mdm2 and relocalize them from the nucleus to the cytoplasm. *J Biol Chem.* 2006;281:21491–21499.
56. Coffa S, Breitman M, Spiller BW, Gurevich VV. A single mutation in arrestin-2 prevents ERK1/2 activation by reducing c-Raf1 binding. *Biochemistry.* 2011;50:6951–6958.
57. Coffa S, Breitman M, Hanson SM, et al. The effect of arrestin conformation on the recruitment of c-Raf1, MEK1, and ERK1/2 activation. *PLoS One.* 2011;6:e28723.
58. Smith WC, Bolch S, Dugger DR, et al. Interaction of arrestin with enolase1 in photoreceptors. *Invest Ophthalmol Vis Sci.* 2011;52:1832–1840.
59. Bychkov ER, Ahmed MR, Gurevich VV, Benovic JL, Gurevich EV. Reduced expression of G protein-coupled receptor kinases in schizophrenia but not in schizoaffective disorder. *Neurobiol Dis.* 2011;44:248–258.
60. Smith TS, Spitzbarth B, Li J, et al. Light-dependent phosphorylation of Bardet-Biedl syndrome 5 in photoreceptor cells modulates its interaction with arrestin1. *Cell Mol Life Sci.* 2013;70:4603–4616.
61. Gurevich VV, Hanson SM, Song X, Vishnivetskiy SA, Gurevich EV. The functional cycle of visual arrestins in photoreceptor cells. *Prog Retin Eye Res.* 2011;30:405–430.
62. Hanson SM, Gurevich EV, Vishnivetskiy SA, Ahmed MR, Song X, Gurevich VV. Each rhodopsin molecule binds its own arrestin. *Proc Natl Acad Sci U S A.* 2007;104:3125–3128.
63. Zuniga FI. Identification of novel protein-protein interactions and functional analysis in the mouse photoreceptor of the hypothetical protein FLJ33482-ALS2CR4 and the small Rho GTPase, Rnd2 [thesis]. Los Angeles, CA: University of Southern California; 2010:1–158.
64. Zuniga FI, Craft CM. Deciphering the structure and function of Als2cr4 in the mouse retina. *Invest Ophthalmol Vis Sci.* 2010;51:4407–4415.
65. Deming JD, Shin J-A, Lim K, Lee E-J, Van Craenenbroeck K, Craft CM. Dopamine receptor D4 internalization requires a beta-Arrestin and a visual Arrestin. *Cell Signal.* 2015;27:2002–2013.
66. Luttrell LM, Gesty-Palmer D. Beyond desensitization: physiological relevance of arrestin-dependent signaling. *Pharmacol Rev.* 2010;62:305–330.

67. Shenoy SK, Lefkowitz RJ. beta-Arrestin-mediated receptor trafficking and signal transduction. *Trends Pharmacol Sci.* 2011;32:521-533.
68. Marchese A, Trejo J. Ubiquitin-dependent regulation of G protein-coupled receptor trafficking and signaling. *Cell Signal.* 2013;25:707-716.
69. Goto Y, Peachey NS, Ripps H, Naash MI. Functional abnormalities in transgenic mice expressing a mutant rhodopsin gene. *Invest Ophthalmol Vis Sci.* 1995;36:62-71.
70. Gorbatyuk M, Justilien V, Liu J, Hauswirth WW, Lewin AS. Suppression of mouse rhodopsin expression in vivo by AAV mediated siRNA delivery. *Vision Res.* 2007;47:1202-1208.
71. Daniele LL, Insinna C, Chance R, Wang J, Nikonov SS, Pugh EN Jr. A mouse M-opsin monochromat: retinal cone photoreceptors have increased M-opsin expression when S-opsin is knocked out. *Vision Res.* 2011;51:447-458.
72. Insinna C, Daniele LL, Davis JA, et al. An S-opsin knock-in mouse (F81Y) reveals a role for the native ligand 11-cis-retinal in cone opsin biosynthesis. *J Neurosci.* 2012;32:8094-8104.
73. Nikonov SS, Kholodenko R, Lem J, Pugh EN Jr. Physiological features of the S- and M-cone photoreceptors of wild-type mice from single-cell recordings. *J Gen Physiol.* 2006;127:359-374.
74. Ogawa Y, Shiraki T, Kojima D, Fukada Y. Homeobox transcription factor Six7 governs expression of green opsin genes in zebrafish. *Proc Biol Sci.* 2015;282.
75. Masuda T, Zhang X, Berlinicke C, et al. The transcription factor GTF2IRD1 regulates the topology and function of photoreceptors by modulating photoreceptor gene expression across the retina. *J Neurosci.* 2014;34:15356-15368.